

# Higher-Order Modulation Formats for Spectral-Efficient High-Speed Metro Systems

R. Freund, M. Nölle, M. Seimetz, J. Hilt, J. Fischer, R. Ludwig, C. Schubert,  
H.-G. Bach, K.-O. Velthaus, M. Schell  
Fraunhofer Institute for Telecommunications, Heinrich-Hertz-Institut,  
Einsteinufer 37, D-10587, Berlin, Germany

## ABSTRACT

Worldwide, higher-order modulation formats are intensively investigated to further increase the spectral efficiency for building the next generation of high-speed metro systems. IQ-modulators, coherent receivers and electronic equalizers are hereby discussed as key devices. We report on system design issues as well as on HHI's latest achievements in developing InP based high-speed modulators and coherent receiver frontends.

**Keywords:** modulation formats, IQ-modulator, coherent receiver, 90° hybrid, InP

## 1. INTRODUCTION

Emerging technologies on the way to 100 Gbit/s line rate and higher spectral efficiency are higher-order modulation formats, coherent receivers and electronic distortion equalizers that permit to operate the next generation of optical transmission systems close to the ultimate limit of spectral efficiency [1]. Higher-order modulation formats encode  $m = \log_2(M)$  data bits on  $M$  states per symbol, which leads to a reduction of the spectral width and allows upgrading to higher data rates with lower-speed components. By employing these new technologies, the complexity of transmitters and receivers increases and a cost reduction has to be achieved by further photonic integration. This cost reduction is expected to play a key role in satisfying the booming bandwidth demand of the future Internet capacity growth at reasonable costs. Figure 1 gives an overview of higher-order modulation formats, such as higher-order phase shift keying (PSK) and quadrature amplitude modulation (QAM) for up to 16 states, intensively investigated for future system applications. These modulation signals can be generated by different transmitter configurations, which differ with respect to their optical and electrical complexity. In principle, a single dual-drive Mach-Zehnder modulator (MZM) is sufficient to generate arbitrary higher-order modulation signals [2], however, higher flexibility is provided by IQ-modulators or a cascade of modulators, which allows to generate high spectral efficient modulation formats using commonly applied binary electrical driving signals.

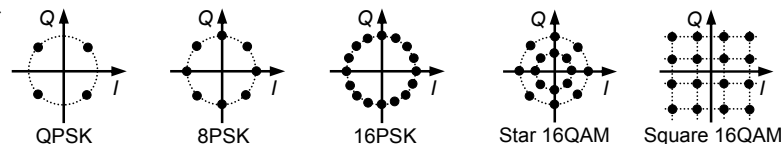


Figure 1. Constellation diagrams of selected higher-order modulation formats (QPSK: quaternary phase shift keying).

Coherent detection is beneficial for systems using higher-order modulation formats because all parameters of the optical field (amplitude, phase, and polarization) are available in the electrical domain and arbitrary modulation formats and constellations can be detected. The preservation of the temporal phase during detection enables the application of efficient methods for the electronic compensation of optical transmission impairments, such as fiber chromatic dispersion, polarization mode dispersion and fiber nonlinearities. A key component for the implementation of coherent detection is the 90° hybrid, which has been recently fabricated at HHI as a monolithically integrated chip on InP [3]. When used in WDM systems, coherent receivers offer tunability and enable very small channel spacings, since channel separation can be supported by highly selective electrical filtering. The main challenges for the practical realization of coherent receivers are the implementation of high-speed analog-to-digital converters, real-time carrier synchronization, electronic equalizers as well as the low cost fabrication of the optical frontend. The next sections describe in more detail transmitter and receiver configurations (s. Section 2 and Section 4), parameter tolerances (s. Section 3) as well as InP based transmitter and receiver components, prototyped by HHI (s. Section 5).

Ronald.Freund@hhi.fraunhofer.de; phone +49 30 31002 652; fax +49 30 31002 250; www.hhi.fraunhofer.de

## 2. TRANSMITTER AND RECEIVER CONFIGURATIONS

Optical higher-order modulation signals can be generated by many different transmitter types, whereby the optical complexity can be reduced through increased electrical complexity and vice versa. In general, higher-order modulation formats are generated in the optical domain by using an optical IQ-modulator. In this case, the necessary number of states of electrical driving signals corresponds to the number of projections of the symbols to the in-phase and quadrature phase. The optical IQ-modulator is a suitable device for generating, e. g., Square QAM signals. However, the generation of multi-level driving signals is required (e.g. quaternary driving signals for Square-16QAM, s. Fig. 2).

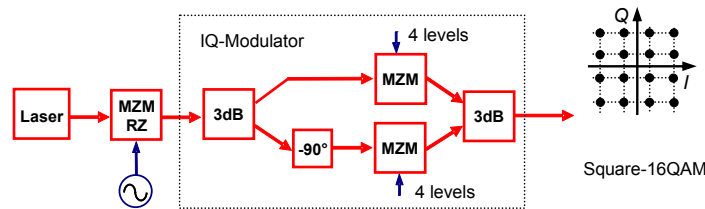


Figure 2. Generation of higher-order modulation formats using multilevel driving signals (RZ: return-to-zero).

Because multi-level electrical driving signals are difficult to generate, especially at high data rates [4], transmitter configurations are attractive, which require solely binary electrical driving signals. However, this increases the number of required optical modulator stages and thus the complexity of the optical transmitter. As an example [5], a simple way for generation of Star-16QAM with binary electrical driving signals is shown in Fig. 3.

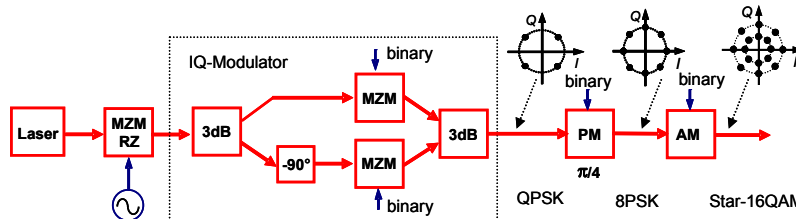


Figure 3. Generation of higher-order modulation formats using binary driving signals (PM: phase modulator, AM: amplitude modulator).

Figure 4 shows the schematic of the coherent receiver, used in next generation optical transmission systems, that consists of an optical frontend, high-speed balanced photodiodes (BD), analog-to-digital converters (ADC) as well as digital signal processing modules, which allow to adaptively compensate for signal distortions. Demodulation of arbitrary high-order modulation signals can be performed completely electrically and compensation of transmission impairments can be accomplished efficiently by digital signal processing. In the case of polarization multiplexing, the optical frontend consists of two optical  $90^\circ$  hybrids, which are used to interfere the received light with the light of a local laser (LO), separately for each of the two orthogonal polarization modes. After detection by balanced photodiodes and analog-to-digital conversion, the received signal is digitally equalized. This signal processing typically comprises timing recovery, adaptive linear and nonlinear equalization, frequency offset and phase correction as well as decoding and data recovery.

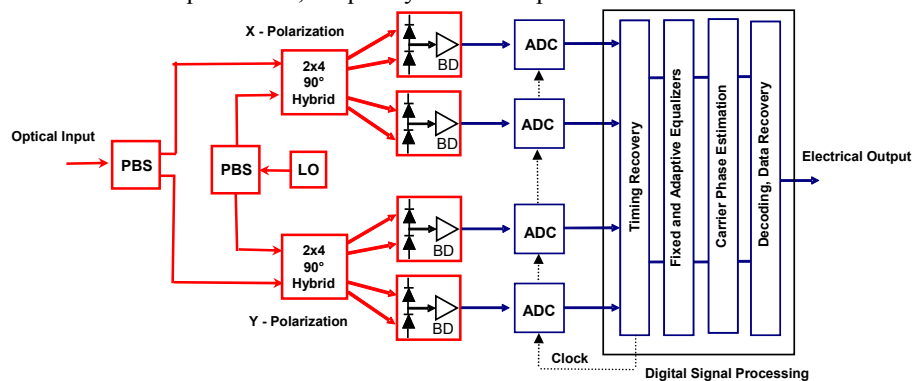


Figure 4. Schematic of the coherent receiver with electronic equalization (PBS: polarization beam splitter).

### 3. SYSTEM TOLERANCES

The migration from traditionally used modulation formats to higher-order formats with more bits per symbol leads to a reduction of symbol rate and spectral width. Therefore, higher spectral efficiencies and per fiber capacities can be achieved. This is the main motivation for system upgrades using higher-order modulation formats. At the same time, migration to higher-order modulation strongly influences the system performance. Positive effects are the improvement of CD tolerances and an increased robustness against PMD due to the reduced symbol rates. Figure 5, left illustrates the CD tolerances of a wide range of modulation formats at a constant bit rate of 112 Gbit/s for RZ pulse shape when homodyne phase estimation receivers without equalization are used. The results were obtained by Monte Carlo simulations using the commercial software tools VPItransmissionMaker and MATLAB. It can be observed that the CD tolerances improve when the order of the modulation format is increased.

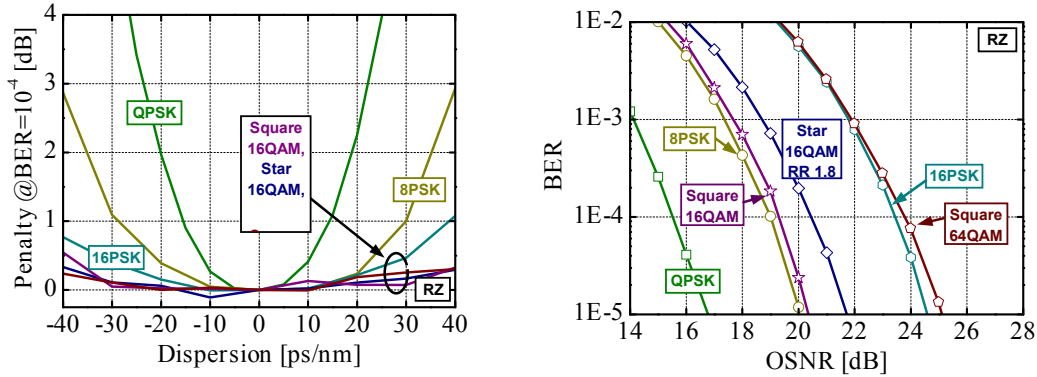


Figure 5. Increase of CD tolerances when migrating to higher-order modulation formats, parameters: homodyne detection with M-th power feed forward digital phase estimation, RZ pulse shape, data rate 112 Gbit/s (left); BER versus received power at 112 Gbit/s for homodyne phase estimation receivers with ideal carrier synchronization for RZ pulse shape (right).

Multi-span long-haul optical fiber transmission systems are typically limited by noise and Kerr nonlinearities. These impairments become more critical for higher-order modulation formats, so that a significantly lower reach is expected when systems are limited by these transmission effects. The noise performance degrades with increasing number of bits per symbol, most significantly for higher-order PSK formats, as shown in Fig. 5, right. QAM formats feature a better noise performance than PSK formats when being compared for the same number of bits per symbol. Figure 6, left illustrates the self phase modulation (SPM) tolerances of various modulation formats, considering 80-km SSMF with linear 100% post-compensation of the CD. Since the phase distances between symbols are getting smaller, the robustness against SPM decreases with increasing order of the PSK format. SPM has a critical impact on QAM signals, in particular, due to the unequal mean nonlinear phase shifts obtained by symbols with different intensity levels. The latter effect can partly be compensated for but is an inherent problem of optical QAM transmission [6]. Tolerances against transmitter- and LO-laser linewidths are shown in Fig. 6, right, applying simple feed-forward phase estimation schemes.

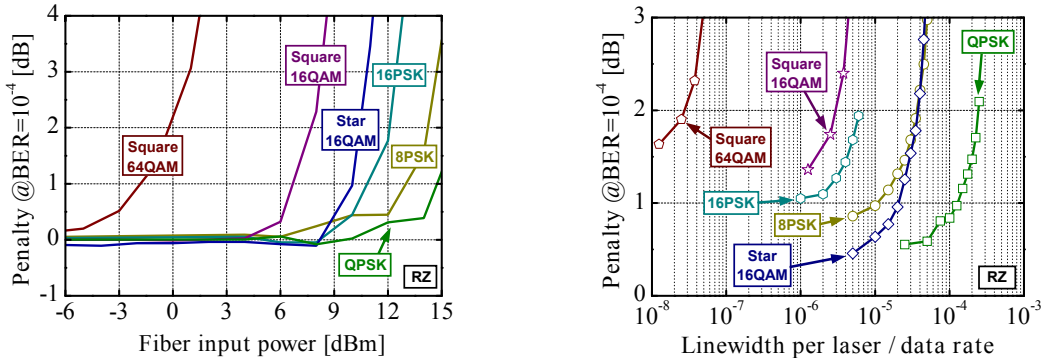


Figure 6. SPM tolerances of various modulation formats for homodyne detection with digital phase estimation at 112 Gbit/s for RZ pulse shape (left); Receiver sensitivity penalties at BER=10<sup>-4</sup> versus the linewidth to data rate ratio for homodyne receivers with feed forward M-th power digital phase estimation (right).

## 4. MULTI-FORMAT TRANSMITTER AND RECEIVER CONCEPTS

Optical higher-order modulation signals can be generated by many different transmitter types (s. Section 2). Figure 7, left shows the block schematic of the digital part of a FPGA-based real-time multi-format transmitter implementation, developed by HHI, which allows the generation of 2PSK, QPSK, and 16QAM data streams with up to 32, 64 and 128 Gbit/s per orthogonal state of polarization, respectively (shown is the 32 Gbaud 16QAM configuration). The transmitter consists of three Virtex-5 FPGAs, where two of them are used to drive the high-speed digital-to-analog converters (DACs) having an amplitude resolution of 6 bit and a sampling-rate of 32 GSa/s.

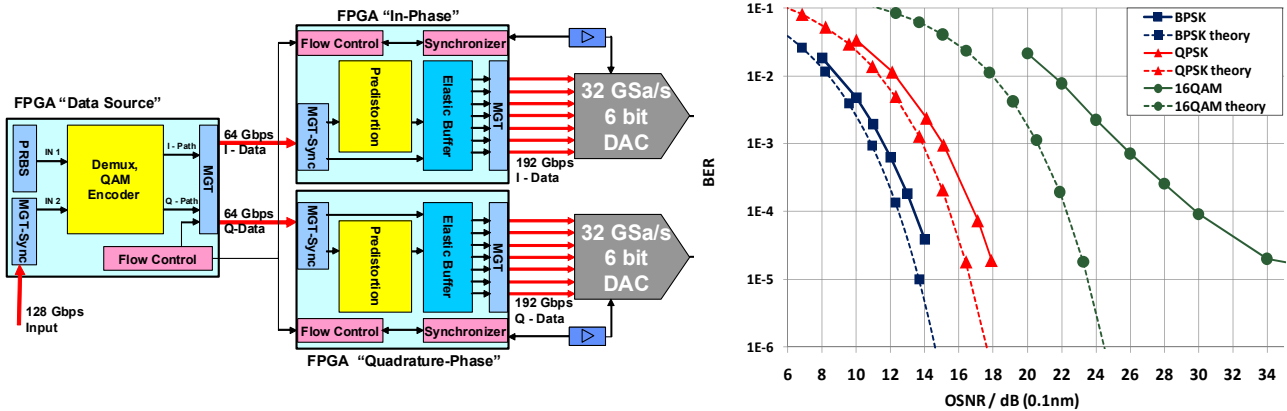


Figure 7. FPGA-based multi-format transmitter (left), back-to-back measured BER vs. OSNR in comparison to theoretical limits for 32 Gbaud 2PSK, QPSK and 16QAM (right), (PRBS: pseudo random bit sequence, MGT: multi-gigabit transceiver).

For data generation, bit mapping and encoding, a separate FPGA board is used. The FPGA design is processing 128 symbols simultaneously. Each FPGA is internally clocked at 250 MHz. The high-speed data transfer between the boards is realized using channel bonded high-speed Rocket-IO interfaces, each clocked at 8.0 Gbit/s. Automatic synchronization of the 64 Rocket-IO interfaces and DACs is implemented with a resolution of 36 ps. The output signals of the DACs are boosted by electrical amplifiers. Electronic pre-distortion is implemented to reduce distortions caused, e.g., by non-ideal output signals of the DACs, non-linear electrical amplification and the non-linear modulator transfer characteristic. Figure 7, right shows back-to-back measured BER vs. OSNR in comparison to theoretical limits for 32 Gbaud 2PSK, QPSK and 16QAM [4].

To overcome the electrical bandwidth limitations of commercially available integrated coherent receiver frontends and electrical ADCs, sampling of the received signal in the optical domain can be applied. This scheme also allows for compensation of optical transmission impairments in the electrical domain despite using lower speed ADCs. The principle of this concept is illustrated for single-polarization signals in Fig. 8.

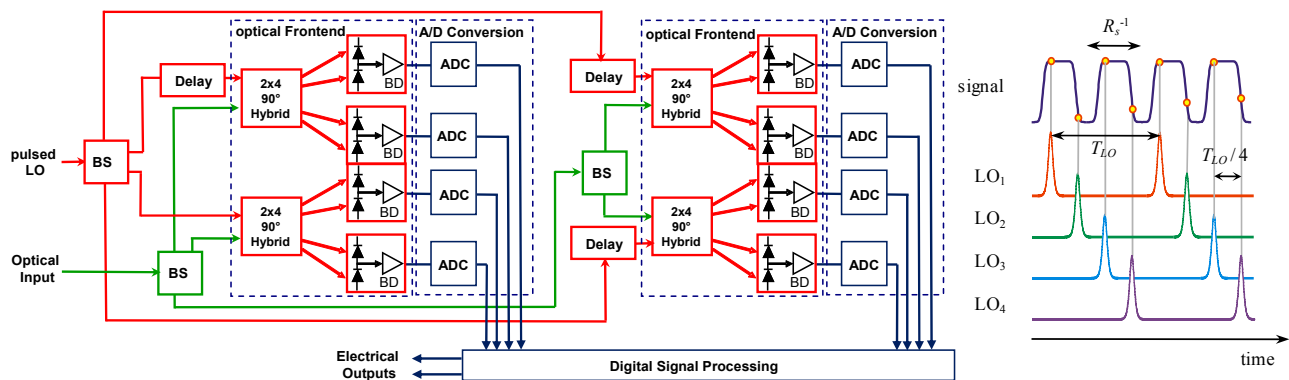


Figure 8. (left) Coherent receiver schematic using high-speed optical sampling and lower speed electronic ADCs (BS: beam splitter, BD: balanced detector), (right) temporal alignment of the delayed sampling pulses ( $R_s$ : symbol rate,  $T_{LO}$ : period between LO pulses).

The received high-speed symbol sequence is sampled in the optical domain by a number of parallel optical samplers - represented by the numbered local oscillator ( $LO_n$ ) sampling pulse trains on the right-hand side of Fig. 8. For the depicted example with four optical samplers, the  $n^{\text{th}}$  LO pulse train has a relative delay of  $(n-1)T_{LO}/4$ , where  $T_{LO}$  denotes the period between LO pulses. Each optical sampler feeds two lower speed ADCs, one for the in-phase and one for the quadrature component of the electric field. This is a scalable architecture which can accommodate arbitrarily high symbol rates as long as the temporal resolution of the optical samplers is sufficiently high. Fig. 9, left compares the required ADC sampling rate (assuming an oversampling ratio of two) for a standard serial coherent receiver and parallel coherent receivers having four, eight and sixteen parallel optical samplers. The parallel optical sampling effectively reduces the required ADC sampling rate.

Since the full electric field is received, the application of digital electronic post-processing, e.g. to compensate for chromatic dispersion or polarization mode dispersion, becomes possible. Sampling the received signal with a sufficient number of samples per symbol avoids the need for an optical clock recovery, which is required for conventional coherent OTDM receivers. Applying this concept, coherent detection of 64 Gbaud (128 Gbit/s) QPSK signals was demonstrated using a configuration with four parallel optical samplers resulting in an aggregate optical sampling rate of 128 GSa/s. This was achieved in spite of only 20 GHz receiver bandwidth and ADCs with a sampling rate of only 50 GSa/s [7,8]. Furthermore, electronic compensation of chromatic dispersion was demonstrated for 56 Gbaud QPSK signals in a transmission experiment over 610 km standard single-mode fiber (SSMF) without any optical dispersion compensation [8]. The measured BER and constellation diagrams are shown in Fig. 9, right. BER performance below the threshold for forward error correction (FEC) with 7% overhead of  $3.8 \times 10^{-3}$  is achieved.

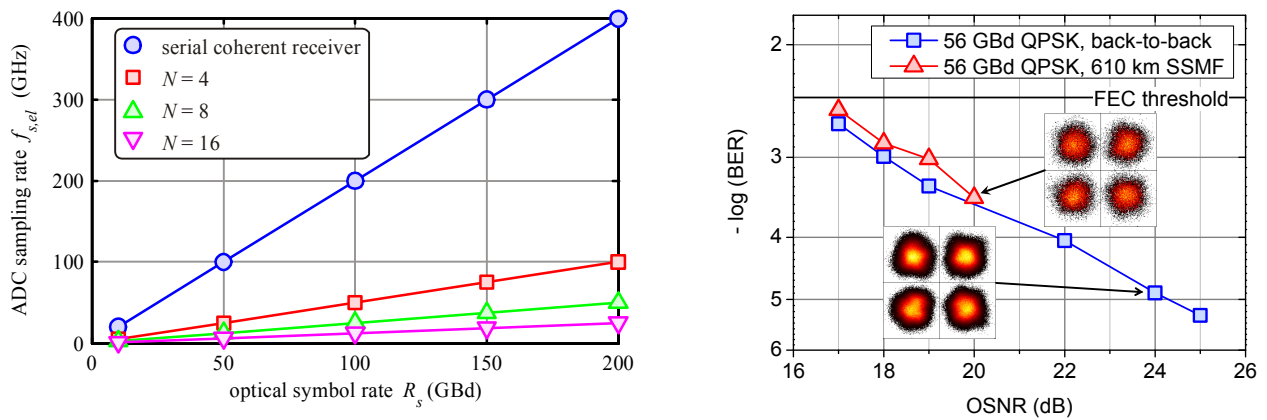


Figure 9. Required ADC sampling rate for different coherent receiver setups (left). BER performance of 56 Gbaud single-polarization QPSK. The coherent receiver uses four optical samplers with an aggregate optical sampling rate of 112 GSa/s. The electrical bandwidth of the receiver is only 20 GHz and the electrical ADCs have a sampling rate of 50 GSa/s (right).

## 5. InP BASED TRANSMITTER AND RECEIVER COMPONENTS

*Highest-speed Mach-Zehnder modulators:* At HHI, InP based modulators are developed based on the travelling wave electrode design (s. Fig. 10, left)[9]. This design approach is the key to achieve a 3-dB bandwidth beyond 50 GHz. By shortening the length of the travelling wave electrodes, Mach-Zehnder devices with even higher bandwidths of up to 63 GHz can be realized but with the drawback of a higher drive voltage of  $\sim 5.5$  Vpp [10,11]. The major advantages of InP MZMs are their compact size, low drive voltage requirements and long-term stability. HHI's InP based MZMs are characterized by a chip bandwidth of up to 53 GHz (s. Fig. 10, right) and a very low drive voltage of  $V_{\pi} = 2.8$  Vpp @ 1550 nm. The achieved optical insertion loss of the packaged module is 4.5-7.0 dB. HHI's MZ modulator structure is suited not only for generation of standard on-off-keying modulation, but also for generation of more enhanced modulation formats, such as differential phase shift keying (DPSK). In a nested structure, IQ-modulators can be built, which allow for the generation of higher-order modulation formats (s. Fig. 2). New developments are focusing on the integration of two nested IQ-modulators. This configuration can be used, e.g. for generation of up to 200 Gbit/s polarization multiplexed QPSK signals.

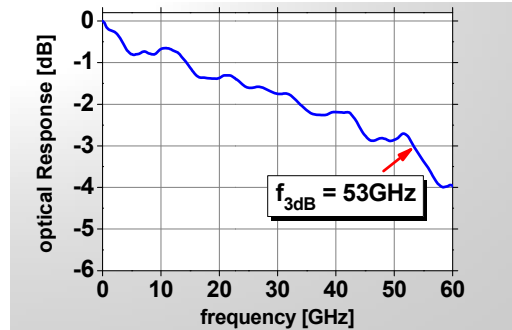
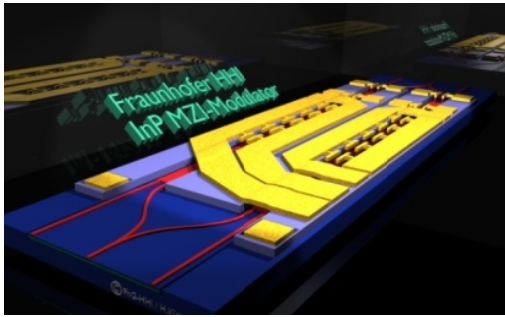


Figure 10. Schematic of an IQ-Modulator (left), bandwidth characteristic of HHI's InP based MZM (right).

*Monolithic 90° hybrid with balanced pin-photodiodes:* Figure 11, top left shows the principle of a 90° hybrid feeding two paired balanced photodetectors. The optical hybrid is designed using a single compact multimode interference coupler (MMI) in a 2x4 I/O configuration. The monolithically integrated device incorporates two optical spot size converters to match the optical field of the input ports to that of a cleaved single-mode fiber. Optical waveguides provide routing of the light from the input tapers via an MMI to the paired balanced photodetectors, thus forming a 2x4 MMI as an optical mixer. The total length of the structure is optimized using an appropriate waveguide design while preserving the high coupling efficiency and low polarization dependent loss (PDL) of the evanescently coupled photodiodes. The total chip size is 5700 x 1300 μm<sup>2</sup>. The fabrication of the optoelectronic integrated circuit (OEIC) starts with MOVPE growth of all optical guiding and waveguiding layers applying semi-insulating GaInAsP/InP layers. The pin-photodiodes of 4.4 x 15 μm<sup>2</sup> size comprise a GaInAs absorption layer and heterostructure contact layers to reach high responsivities and high bandwidths [12]. Figure 11, bottom left depicts the realized OEIC. The two heating elements at the left side have been added as phase shifters to simplify the measurement setup and are not required in a final product. Reverse leakage of the four pin-detectors amounts to less than 5 nA at 2 V bias. The achieved RF-bandwidth is > 60 GHz [13]. The OEIC was fully packaged (s. Fig. 11, right) for extensive characterizations over wavelength and temperature. Stable performance was achieved over a wavelength range from 1520 nm to 1570 nm and a temperature range from 0°C to 75°C.

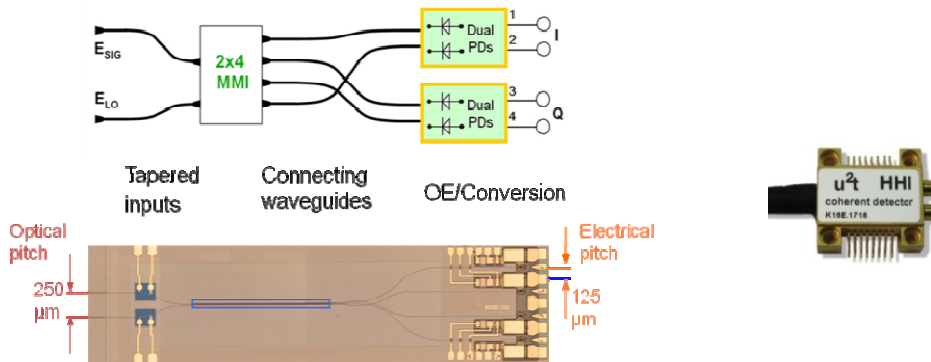


Figure 11. Schematic of the 90° hybrid with two integrated balanced photodetectors (top left), structure of the chip (bottom left), packaged 90° hybrid (right).

*Integrated coherent receiver module:* The core components of the integrated receiver module are two optical 90° hybrids, each monolithically integrated with four waveguide-integrated pin-photodiodes in balanced configuration. The 90° hybrids with the integrated pin-photodiodes are co-packaged into one module with four differential transimpedance amplifiers (TIA), used for linear amplification of the received signal up to differential output voltages of > 1 V<sub>pp</sub>. Figure 12, left shows the block diagram of a setup for coherent reception of a polarization multiplexed signal. The dashed rectangle indicates the co-packaged parts that are included in the coherent receiver module. The optical polarization beam splitter (PBS) and the beam splitter (BS) for combining the local oscillator (LO) with the incoming data signal (SIG) are not included in the receiver module. The package utilizes a coplanar waveguide RF-interface for surface mount assembly of the device. The optical hybrids have been designed using a single, highly compact MMI in a

2x4 I/O configuration, as described in the last subsection. The 3 dB cut-off frequency of the device was found to be around 26 GHz for all outputs [14], including the TIAs. In the time domain, the phase deviation between I and Q channels in the 90° hybrid has been characterized using a real-time digital oscilloscope capturing all I/Q outputs simultaneously and evaluating the phase difference and skew over a wavelength range from 1530 nm to 1570 nm. The device showed very low phase error of less than  $\pm 5^\circ$  over the full C-band wavelength range and up to a module temperature of 75°C [14]. Figure 12, right shows the BER performance and received constellation diagrams of the integrated coherent receiver in a back-to-back (b2b) experiment with 40 Gbaud single and dual-polarisation (DP) QPSK signals as well as in a transmission experiment with 40 Gbaud (160 Gbit/s) DP-QPSK signals transmitted over 610 km of standard single-mode fibre (SSMF) [15].

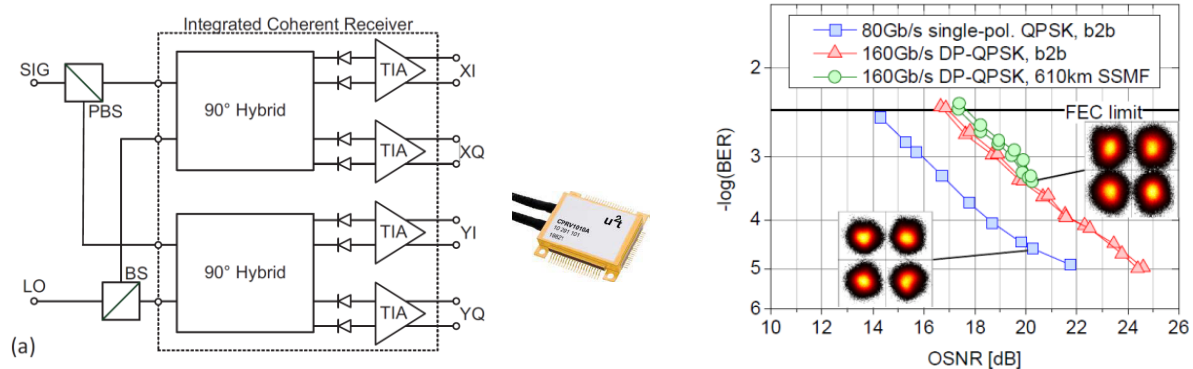


Figure 12. Structure of the integrated coherent receiver and packaged module (left), performance characteristic of the integrated coherent receiver for 40 Gbaud QPSK (right).

## 6. CONCLUSION

Higher-order modulation formats are intensively investigated to further increase the spectral efficiency in next generation high-speed metro systems. IQ-modulators and coherent receivers are hereby the key device for generation and detection, respectively, of higher order modulation formats. HHI developed an InP based MZM (RF-bandwidth > 53 GHz,  $V\pi = 2.8$  Vpp @ 1550 nm) and a monolithically integrated optoelectronic circuit that consists of a 90° hybrid and two balanced pin-photodiodes (RF-bandwidth > 60 GHz). This OEIC is the key device of a recently demonstrated integrated coherent receiver that paves the way to compact receiver devices at affordable prices.

## 7. ACKNOWLEDGEMENT

This work has been partly funded by the German Ministry of Education and Research in the framework of the Celtic project 100GET and in the program Optical Technologies under contract number 13N9356 as well as by the European Network of Excellence EURO-FOS. For the receiver work, the cooperation with u2t Photonics AG is highly appreciated, by contributing to packaging, specifications and characterization of the devices.

## REFERENCES

- [1] J.M. Kahn, K.P. Ho, "Spectral Efficiency Limits and Modulation/ Detection Techniques for DWDM Systems", IEEE Journal of Selected Topics in Quantum Electronics, 10(2) 2004, pp. 259-272.
- [2] K.P. Ho, H.W. Cui, "Generation of arbitrary quadrature signals using one dual-drive modulator", IEEE Journal of Lightwave Technology, 23(2) 2005, pp. 764-770.
- [3] H.G. Bach, A. Matiss, C.C. Leonhardt, R. Kunkel, D. Schmidt, M. Schell, A. Umbach, "Monolithic 90°Hybrid with Balanced PIN Photodiodes for 100 Gbit/s PM-QPSK Receiver Applications", Proc. Optical Fiber Communication Conference (OFC 2009), San Diego (USA), 22-26 March 2009, paper OMK5.
- [4] J. Hilt, M. Nölle, L. Molle, M. Seimetz, R. Freund, "32 Gbaud Real-Time FPGA-Based Multi-Format Transmitter for Generation of Higher-Order Modulation Formats", Proc. 9th International Conference on Optical Internet (COIN 2010), Jeju (Korea), 11-14 July 2010.
- [5] M. Seimetz, R. Freund, "Next Generation Optical Networks Based on Higher-Order Modulation Formats, Coherent Receivers and Electronic Distortion Equalization", Elektrotechnik und Informationstechnik: E & I, 125(2008)7/8, pp. 284-289.

- [6] M. Seimetz, "High-Order Modulation for Optical Fiber Transmission", Springer Series in Optical Sciences, Vol. 143, ISBN 978-3-540-93770-8, Springer, 2009.
- [7] J.-K. Fischer, R. Ludwig, L. Molle, C. Schmidt-Langhorst, A. Galperin, T. Richter, C. Leonhardt, A. Matiss, C. Schubert, "High-Speed Digital Coherent Receiver with Parallel Optical Sampling", Proc. Optical Fiber Communication Conference (OFC 2010), San Diego (USA), 21-25 March 2010, post-deadline paper PDPB4.
- [8] J. K. Fischer, R. Ludwig, L. Molle, C. Schmidt-Langhorst, C. C. Leonhardt, A. Matiss, C. Schubert, "Digital Coherent Receiver Based on Parallel Optical Sampling", Proc. 36th European Conference on Optical Communication (ECOC 2010) , Turin (Italy), September 19-23 2010, paper Th.10.A.4.
- [9] H.N. Klein, H. Chen, D. Hoffmann, S. Staroske, A.G. Steffan, K.O. Velthaus, "1.55 $\mu$ m Mach-Zehnder Modulators on InP for optical 40/80 Gbit/s transmission networks", Proc. 18th Int. Conf. InP and Related Materials (IPRM 2006), Princeton (USA), 7-11 May 2006, paper TuA2.4.
- [10] K.O. Velthaus, H.-G. Bach, "High-speed Integrated Modulators and Receivers", Proc. Integrated Photonics and Nanophotonics Research and Applications (IPNRA 2007), Salt Lake City (USA), July 8-11 2007, paper IMA5.
- [11] H. Chen, H.N. Klein, D. Hoffmann, K.O. Velthaus, H. Venghaus, "Improvement Strategy towards 80 Gbit/s Low Drive Voltage InP based Mach-Zehnder Modulator", 4th Joint Symposium on Opto- and Microelectronic Devices and Circuits (SODC 2006), Duisburg (Germany), 3-8 September 2006.
- [12] A. Beling, H.G. Bach, D. Schmidt, G.G. Mekonnen, M. Rohde, L. Molle, H. Ehlers, A. Umbach "High-Speed Balanced Photodetector Module with 20dB Broadband Common-Mode Rejection Ratio", Proc. Optical Fiber Communication Conference (OFC 2003), Atlanta (USA), 23-28 March 2003, paper WF4.
- [13] R. Kunkel, H.-G. Bach, D. Hoffmann, G.G. Mekonnen, R. Zhang, D. Schmidt, and M. Schell, "Athermal InP-Based 90°-Hybrid Rx OEICs with pin-PDs >60 GHz for Coherent DP-QPSK Photoreceivers", Proc. 22th Int. Conf. InP and Related Materials (IPRM 2010), 31 May - 4 June 2010, Takamatsu (Japan), paper FrA1-2.
- [14] A. Matiss, R. Ludwig, J.-K. Fischer, L. Molle, C. Schubert, C.C. Leonhardt, H.G. Bach, R. Kunkel, A. Umbach, "Novel Integrated Coherent Receiver Module for 100G Serial Transmission", Proc. Optical Fiber Communication Conference (OFC 2010), San Diego (USA), 21-25 March 2010, paper PDPB3.
- [15] R. Ludwig, J. K. Fischer, A. Matiss, L. Molle, C. C. Leonhardt, H.-G. Bach, R. Kunkel, A. Umbach, C. Schubert, "Performance of a Novel Integrated Coherent Receiver Module for 100G Ethernet Applications and Beyond", Proc. 36th European Conference on Optical Communication (ECOC 2010), Turin (Italy), September 19-23 2010, paper Mo.2.F.1.